Title

Isomer-specific kinetics of the C+ + H2O reaction at the temperature of interstellar clouds

Journal

Science Advances, 7(2)

ISSN

2375-2548

Authors

Yang, Tiangang
Li, Anyang
Chen, Gary K
et al.

Publication Date

2021-01-06

DOI

10.1126/sciadv.abe4080

Peer reviewed

PLANETARY SCIENCE

Isomer-specific kinetics of the $C^+ + H_2O$ reaction at the temperature of interstellar clouds

Tiangang Yang[1,2]*, Anyang Li[3]*, Gary K. Chen[1], Qian Yao[4], Arthur G. Suits[5], Hua Guo[4]†, Eric R. Hudson[1,6]†, Wesley C. Campbell[1,6]†

The reaction $C^+ + H_2O \rightarrow HCO^+/HOC^+ + H$ is one of the most important astrophysical sources of HOC^+ ions, considered a marker for interstellar molecular clouds exposed to intense ultraviolet or x-ray radiation. Despite much study, there is no consensus on rate constants for formation of the formyl ion isomers in this reaction. This is largely due to difficulties in laboratory study of ion-molecule reactions under relevant conditions. Here, we use a novel experimental platform combining a cryogenic buffer-gas beam with an integrated, laser-cooled ion trap and high-resolution time-of-flight mass spectrometer to probe this reaction at the temperature of cold interstellar clouds. We report a reaction rate constant of $k = 7.7(6) \times 10^{-9}$ cm^3 s^{-1} and a branching ratio of formation $\eta = HOC^+/HCO^+ = 2.1(4)$. Theoretical calculations suggest that this branching ratio is due to the predominant formation of HOC^+ followed by isomerization of products with internal energy over the isomerization barrier.

INTRODUCTION

Stars and their accompanying solar systems are born from dense, cold molecular clouds that host an unexpectedly rich and complex chemistry (*1*). This chemistry is largely driven by intense ultraviolet (UV) radiation from nearby massive young stars in so-called photon-dominated regions (PDRs) on the surface of such clouds (*2*), by cosmic rays that penetrate deep into the clouds in regions opaque to UV light or, in some cases, by x-ray–dominated regions (XDRs) from the circumnuclear disks (CNDs) of active galactic nuclei (AGNs) containing supermassive black holes (*3*, *4*). This complex chemistry then seeds newly formed solar systems, and the process continues in successive generations of star formation and demise.

The chemistry within these clouds sensitively reflects the local conditions of radiation exposure, temperature, density, structure, and dynamics. With the advent of interferometric radio telescopes such as NOEMA (NOrthern Extended Millimeter Array) and ALMA (Atacama Large Millimeter/submillimeter Array) and others that can image specific molecules at unprecedented spatial resolution (*5*, *6*), the broad-brush view of these diverse environments is giving way to rich detail for probing and cataloging their structure, composition, and local conditions, even in distant galaxies. An understanding of the associated chemistry is essential to build accurate models and also identify species that are reliable tracers for conditions such as UV or x-ray irradiation. Laboratory experiments that can investigate specific reactions under conditions resembling those in low-density interstellar clouds at 10 to 50 K are essential to develop these models and identify suitable reporter molecules, complementing the enormous investment in the observational tools.

Advanced experimental techniques developed in atomic physics for preparation of ultracold matter and quantum information science have recently been adapted to chemical studies. While these techniques allow preparation and coherent control of a reagent in single internal and external quantum states, they have, so far, been limited to a narrow range of species, e.g., the alkali atoms. As a result, despite groundbreaking work that has assembled single molecules (*7*), observed a conformer-dependent reaction (*8*), and produced novel molecules (*9*), no study to date has adapted these techniques to a reaction where all reagents are chemically relevant. Here, we develop a novel experimental platform based on these atomic physics techniques that allows studies of reactions of virtually any atomic ion with a wide range of neutral molecules. Specifically, we combine a laser-cooled ion trap with integrated mass spectrometer (MS) and cryogenic buffer-gas beam (CBGB) (Fig. 1A). These tools have been independently used in a number of pioneering studies (*8*–*12*), but they have typically been restricted to laser-cooled atomic reagents and produce reagents at temperatures substantially colder than the interstellar medium (ISM). In this work, we adapt them to produce C^+ and H_2O at more characteristic temperatures (≈20 K) to properly simulate cold interstellar clouds in the laboratory.

Using this platform, we study the reaction $C^+ + H_2O \rightarrow HOC^+/HCO^+ + H$ with product isomer specificity under conditions relevant to those in cold molecular clouds. This reaction is believed to be the chief source of the metastable ion HOC^+, which has been observed in a variety of sources including of nearby PDRs (*13*), toward our own galactic center (*14*, *15*), in the early starburst galaxy M82 (*16*, *17*), a later starburst galaxy NGC 253 (*18*), in the ultraluminous infrared galaxy Mrk273 (*19*), and in the AGNs of NGC 1068 and other active galaxies. The lower-energy isomer HCO^+, on the other hand, is largely formed via protonation of CO by the ubiquitous ion H_3^+, and it is generally far more abundant. The relative abundance of HCO^+ to HOC^+ is seen to vary by many orders of magnitude, from well over 10^4 in the weakly irradiated PDR S140 (*13*) to 10 in the inner CND of Mrk273 (*19*). One question is, To what extent can HOC^+ serve as a specific marker for XDRs (*3*)? A recent survey toward two quiescent cloud complexes of the galactic center, one of which is likely exposed to strong x-ray radiation, suggested that the CS:HOC^+ ratio was a reliable marker for PDR/XDR components in

[1]Department of Physics and Astronomy, University of California, Los Angeles, Los Angeles, CA 90095, USA. [2]Department of Chemistry, Southern University of Science and Technology, Shenzhen 518055, P. R. China. [3]Key Laboratory of Synthetic and Natural Functional Molecule Chemistry, Ministry of Education, College of Chemistry and Materials Science, Northwest University, Xi'an 710127, P. R. China. [4]Department of Chemistry and Chemical Biology, University of New Mexico, Albuquerque, NM 87131, USA. [5]Department of Chemistry, University of Missouri, Columbia, MO 65211, USA. [6]UCLA Center for Quantum Science and Engineering, University of California, Los Angeles, Los Angeles, CA 90095, USA.
*These authors contributed equally to this work.
†Corresponding author. Email: wes@physics.ucla.edu (W.C.C.); eric.hudson@ucla.edu (E.R.H.); hguo@unm.edu (H.G.)

galactic nuclei exposed to large-scale shocks, but there was no molecular tracer useful to distinguish PDR and XDR regions (*20*). For models to be used reliably to reveal conditions in distant molecular clouds in these very diverse environments, the yield of the associated reactions must be accurately known. These relative abundances obviously depend on the product branching ratios of the underlying chemical reactions that produce these molecules (*13*, *21*). For the title reaction, the product channels are

$$C^+ + H_2O \rightarrow HOC^+ + H \quad (1)$$

$$C^+ + H_2O \rightarrow HCO^+ + H \quad (2)$$

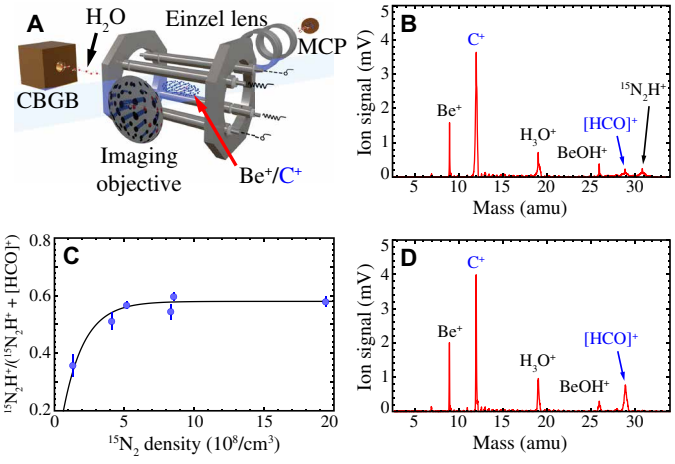

Fig. 1. Measurement of the reaction rate and isomeric branching ratio. (**A**) Schematic diagram of the experimental setup. MCP, Micro-channel Plate. (**B**) Time-of-flight trace (10 sample average) of Be^+ and C^+ exposed to water from the CBGB and $^{15}N_2$ from the leak valve (10 s) at a density of 1×10^9 cm^{-3}. amu, atomic mass units. (**C**) The fraction of the titrated isomers saturating as a function of $^{15}N_2$ density. Fitted parameters yield a ratio of trapped reaction products of 1.4(2) and $k_3 = ((6.6 \pm 1.0) \times 10^{-10})$ cm^3/s. (**D**) Same as (B), but with 20 s of $C^+ + H_2O$ reaction and isomerization via CO introduced as a background gas before titration with N_2. The lack of a peak for $^{15}N_2H^+$ indicates that the CO has converted all of the HOC^+ to HCO^+ and that HOC^+ does not react with N_2.

Hence, the rate and branching ratio, $\eta = HOC^+/HCO^+$, of this reaction has attracted significant interest over the past 30 years; however, there is still no consensus on the latter value and it has never been measured at low temperature (*22*–*26*). Freeman and McEwan (*22*) investigated this reaction with a selected-ion flow tube (SIFT) at room temperature and reported $\eta \approx 5(2)$ by using the different proton transfer rates of the isomers with N_2O to distinguish HCO^+ from HOC^+. Martinez and co-workers (*27*) more recently studied the reaction using the flowing-afterglow-SIFT technique to eliminate the contribution of electronically excited C^+ ions but did not measure branching and quite reasonably assigned all the products to HOC^+. Sonnenfroh *et al.* (*25*) carried out a crossed-beam experiment to study this reaction at collision energies of 0.62 and 2.14 eV, in which they concluded that $\eta \leq 2.3$ and pointed out that the high internal temperature of the products due to the exothermicity of the reaction ($\Delta H = -4.34$ eV) may affect the identification of the isomers in subsequent titration reactions. In theoretical calculations, Defrees *et al.* (*28*) used phase-space arguments to calculate $\eta = 2$. However, using quasi-classical trajectory (QCT) studies, Ishikawa *et al.* (*29*) found that HOC^+ dominated the initial products of the reaction giving $\eta \approx 100$. The authors discussed the possibility of subsequent isomerization due to internal energy of the products to explain the existence of HCO^+ in experimental observations; however, no calculations for the isomerization rate were performed. Despite these disagreements, the room temperature measurement of η (*22*) has been widely used to understand ISM chemistry and classify PDRs for decades (*13*).

Here, we build on pioneering work of Gerlich and others (*30*–*32*) and report the first study of the $C^+ + H_2O$ reaction under conditions present in cold molecular clouds of the ISM. We find the reaction proceeds with a rate constant of $k = 7.7(6) \times 10^{-9}$ cm^3 s^{-1} at ≈20 K, slightly lower than the value reported at 27 K (*26*). Titrating the reaction products with $^{15}N_2$, which reacts with HOC^+ but not HCO^+, we measure the ratio of HOC^+ to HCO^+ exposed to the titrant to be 1.4(2). Accounting for isomerization during the titration process, we report $\eta = 2.1(4)$. QCT calculations on an accurate potential energy surface (PES) found that the $C^+ + H_2O$ reaction produces 97.6% HOC^+, of which 87.8% of these products are produced with an internal energy above the isomerization barrier. We calculate that the

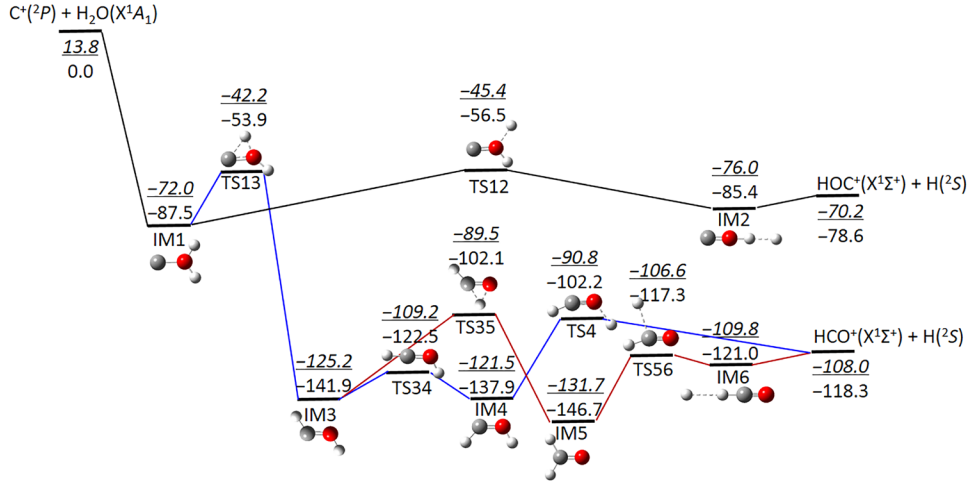

Fig. 2. Energetics of the ground-state reaction pathways for the $C^+ + H_2O$ reaction. The relative energies are marked, along with the ZPE (Zero Point Energy)–corrected values (italic and underlined) in kilocalorie per mole.

density of HOC^+ vibrational states is twice that of HCO^+ near the isomerization barrier. Therefore, we expect that roughly two-thirds of the above-barrier products decay to HOC^+, which modifies the predicted branching ratio to $\eta = 2.3$, in agreement with the experiment.

MATERIALS AND METHODS

A schematic of the apparatus used in this study is shown in Fig. 1A. Briefly, an integrated laser-cooled ion trap and time-of-flight (TOF)–MS (*33*), which has been described in detail elsewhere (*34*, *35*), is combined with a CBGB (*18*). Laser ablation of beryllium and graphite is used to simultaneously produce Be^+ and C^+ ions, which are trapped in a linear radio frequency Paul trap. Laser cooling (*36*) is used to cool the translational motion of the Be^+ ions, which sympathetically (*37*, *38*) cools the cotrapped C^+ ions to <1 K. This process takes several seconds; during that time, any metastable (^4P) C^+, which may have plagued other measurements as explained in (*27*), spontaneously relaxes (*39*). Water vapor is entrained in the neon CBGB (*40*), which is cooled by a closed-cycle refrigerator to 20.0(5) K, and directed toward the center of the ion trap with a forward velocity of 150(2) m/s (see the Supplementary Materials) to facilitate $C^+ + H_2O$ reactions. The reactions occur inside the ion trap, which is held in a high vacuum chamber ($<5 \times 10^{-10}$ mbar) (*34*, *35*), and the trapped ionic reactants and products are analyzed by an integrated TOF-MS (*9*, *41*, *42*).

Two isomers of the formyl ion, HCO^+ and HOC^+, are produced in this reaction; however, TOF-MS is unable to distinguish these ions as they have the same mass and charge. To distinctly titrate the HCO^+ from the HOC^+, a third gas with proton affinity between the two isomers is introduced. Specifically, N_2 is chosen because of its low reactivity with other trapped species, instead of N_2O or other gases with suitable proton affinity (*22*) (see the Supplementary Materials), to simplify the analysis of the titrated products. The titration reactions of interest are

$$HOC^+ + N_2 \rightarrow N_2H^+ + CO \quad (3)$$

$$HCO^+ + N_2 \rightarrow \text{No reaction} \quad (4)$$

Unfortunately, the mass of diazenylium ($^{14}N_2H^+$), $m_D = 29.01$ atomic mass units (amu), is nearly equal to that of the formyl ion, $m_F = 29.00$ amu, and these products cannot be resolved by our MS. Therefore, we use $^{15}N_2$ as a titrant gas to produce diazenylium with a mass of 31.01 amu, which is easily resolved by our MS. Reaction 4 has been validated experimentally, as shown in Fig. 1D.

The experimental sequence is described in the Supplementary Materials. Briefly, trapped C^+ ions are sympathetically cooled by the cotrapped Be^+ ions. Next, the H_2O beam is introduced into the trap for 20 s and reactions occur. After an approximately 1-s delay to allow the internally excited product ions to isomerize and/or relax via radiative decay (*43*), the $^{15}N_2$ titrant gas is introduced for approximately 10 s. Afterward, all ions are ejected into the TOF-MS, and Fig. 1B shows a typical TOF signal. From these data, we find the reaction rate constant $k_1 + k_2 = 7.7(6) \times 10^{-9}$ cm^3 s^{-1} (see section S3 for the details).

Several other species, not studied here, are also apparent in the TOF-MS signal. These are understood as follows. Be^+ ions are known to react with H_2O to make $BeOH^+$ and a small amount of H_3O^+ (*34*, *35*). Most of the H_3O^+ comes from the reactions

$$HCO^+ + H_2O \rightarrow H_3O^+ + CO \quad (5)$$

$$HOC^+ + H_2O \rightarrow H_3O^+ + CO \quad (6)$$

The rate coefficient of reaction 5 has been measured as $(2.5 \pm 0.3) \times 10^{-9}$cm^3/s at 300 K (*44*), but not at lower temperature. Although the appearance of H_3O^+ presents no problem for our study, a relative rate difference between these two reactions (5 and 6) at low temperature would systematically shift the trapped HOC^+/HCO^+ ratio and cause an error in the determination of branching ratio η. To constrain this potential error, we introduced CO to produce samples with varying compositions of HCO^+ and HOC^+ (details can be found in the Supplementary Materials) from the reaction

$$HOC^+ + CO \rightarrow HCO^+ + CO \quad (7)$$

We find $k_5 \approx k_6 = (1.7 \pm 0.2) \times 10^{-8}$cm^3/s, and therefore, the HOC^+/HCO^+ ratio is not measurably affected.

Therefore, since isomerization of the isoformyl ion by H_2O does not occur (*45*) (see the Supplementary Materials), the branching ratio of HOC^+ and HCO^+ can be inferred from the ratio of the integrated mass/charge ratio (m/z) = 31.01 amu/e ($^{15}N_2H^+$) and m/z = 29.00 amu/e (HCO^+) peaks in the TOF signal, which is found to be 1.4(2). Repeating this process over various densities (Fig. 1C) of $^{15}N_2$ allows us to confirm this measurement as well as determine the proton transfer rate constant of reaction 3 to be $k_3 = 6.6(1) \times 10^{-10}$cm^3/s (see the Supplementary Materials).

In addition, to verify that $^{15}N_2$ is only able to react with HOC^+ and not HCO^+. We repeat the above process in the presence of a large amount of neutral CO gas for converting all of the HOC^+ to HCO^+ via the isomerization reaction 7 and then introduce excess $^{15}N_2$. Since there is no evidence of m/z = 31.01 amu/e ($^{15}N_2H^+$) in the TOF trace (Fig. 1D), reactions 3 and 4 are validated.

RESULTS

Before the branching ratio η can be extracted from the measured product ratios, it is necessary to account for isomerization by the titrant gas, i.e.

$$HOC^+ + {}^{15}N_2 \rightarrow HCO^+ + {}^{15}N_2 \quad (8)$$

As HCO^+ is unreactive to $^{15}N_2$ at these temperatures, this reaction artificially lowers the measured branching ratio. To understand this effect, QCT calculations (*46*) on an long-range corrected ab initio PES for the $HOC^+ + N_2$ system were performed (*47*). These calculations yield a 14% isomerization (see the Supplementary Materials) fraction. The isomerization fraction can be constrained with the assumption that the total rate constant for $HOC^+ + {}^{15}N_2$ is given by the Langevin capture rate constant, $k_L = 8.0 \times 10^{-10}$ cm^3/s. Thus, the measured value of k_3 suggests a possible isomerization fraction of up to 18%. Using the isomerization rate found in the QCT calculations, the measured reaction branching ratio becomes $\eta = 2.1(4)$.

DISCUSSION

To better understand this reaction, a six-dimensional global PES for reactions 1 and 2 was constructed from the explicitly correlated unrestricted coupled cluster singles, doubles, and perturbative triples [UCCSD(T)-F12a] calculations (details of ab initio calculations and fitting are given in the Supplementary Materials). The energetics for

reactions 1 and 2 are shown in Fig. 2. As C^+ approaches water, it can be transiently trapped in the IM1 (Intermediate 1) well, in which C is bonded to O. Given the system energy, however, the intermediate is relatively short lived and not significantly affected by the two transition states. Because of the large frequency mismatch among its vibrational modes, the vibrational energy is hardly randomized in the intermediate. In most cases, the large energy in the C—O mode is quickly transferred to an OH bond, leading to its cleavage and resulting in the HOC^+ product. In a small number of trajectories, however, the energy transfer is not sufficient to dissociate the H but allows the H to undergo large amplitude motion around the HOC moiety, leading to the formation of HOCH intermediates (IM3, IM4, and IM6). Eventually, the dissociation of the O—H bond results in the formation of HCO^+. Two exemplary trajectories are illustrated in fig. S7. The large HOC^+/HCO^+ branching ratio is a testament of the nonstatistical nature of the reaction.

The QCT calculations performed on the PES using the experimental conditions with a total of 48,656 trajectories found that the thermal rate constant and branching ratio are $k_1 + k_2 = (5.02 \pm 0.03) \times 10^{-9}$cm^3/s and $\eta = 40.5 \pm 2.0$, respectively. While the rate constant is in reasonable agreement with the measured value, the branching ratio is ≈20 times larger. However, because reactions 1 and 2 are quite exothermic, 87.8% (29.6%) of the HOC^+ (HCO^+) is produced with internal energy above the isomerization barrier. As a result, as the product molecules radiatively cool, η can change markedly. Since this cooling proceeds via vibrational decay, the isomerization fraction can be estimated via the density of vibrational states of each isomer near the barrier (see the Supplementary Materials). Primarily, because of the lower vibrational frequency of the HOC^+ bending mode, it exhibits ≈2× higher density of states near the isomerization barrier, indicating that roughly two-thirds (one-third) of the above-barrier products will decay to HOC^+ (HCO^+). Thus, the radiative cooling process lowers the QCT-calculated branching ratio to $\eta \approx 2.3$, in agreement with the experimental value.

Thus, the agreement of the present measurement of the branching ratio with that predicted by phase-space theory (*28*) is potentially misleading. The reaction is not statistical but direct and is followed by radiative cooling that substantially alters the end product ratio. This view is consistent with crossed molecular beam experiments from Farrar and co-workers (*25*) at high collision energies. They mapped the product velocity distributions on a microsecond time scale and noted that the angular distribution was asymmetric, suggesting a lifetime for the transient intermediate on the order of a rotational period, $\approx 10^{-13}$ s. We note that one of the unique features of the present approach as compared to previous work on the $C^+ + H_2O$ reaction is the capability to permit the products to relax fully before detection, as would occur in low-density conditions in the ISM.

Summary

We report the use of a recently developed tool, a CBGB coupled to an integrated ion trap and MS, to simulate conditions in the cold ISM in the laboratory. We use this tool to study the $C^+ + H_2O \rightarrow HCO^+/HOC^+ + H$ reaction, finding a reaction rate constant [$k = 7.7(6) \times 10^{-9}$ cm^3 s^{-1}] and branching ratio [$\eta = HOC^+/HCO^+ = 2.1(4)$] that can correct inconsistencies in the models (*48*, *49*). QCT calculations on a highly accurate PES reveal the reaction proceeds by a direct mechanism to overwhelmingly (97.6%) produce HOC^+. However, because of the large exothermicity of the reaction, the internal energy of a majority (87.8%) of these products is larger than the isomerization barrier. During radiative cooling, ~$^1/_3$ of the above-barrier HOC^+ is expected to isomerize to HCO^+, lowering the predicted branching ratio to $\eta = 2.3$.

Interstellar molecular clouds ultimately yield the seedbed from which new stars and planets are born, as well as the raw materials from which life likely developed. Thus, understanding the chemical evolution of the ISM is essential to understanding these important processes. Chemical reaction rates and branching ratios underlying models of this evolution are often (necessarily) taken from experiments and theory that are not appropriate for the conditions present in cold molecular clouds. The apparatus used here is quite versatile and could be applied in its present form to study most atomic ion–neutral molecule reactions under conditions relevant to cold molecular clouds of the ISM chemistry.

SUPPLEMENTARY MATERIALS

Supplementary material for this article is available at http://advances.sciencemag.org/cgi/content/full/7/2/eabe4080/DC1

REFERENCES AND NOTES

1. Y. Aikawa, V. Wakelam, R. T. Garrod, E. Herbst, Molecular evolution and star formation: From prestellar cores to protostellar cores. *Astrophys J.* **674**, 984–996 (2008).
2. D. J. Hollenbach, A. G. G. M. Tielens, Photodissociation regions in the interstellar medium of galaxies. *Rev. Mod. Phys.* **71**, 173–230 (1999).
3. A. Usero, S. García-Burillo, A. Fuente, J. Martín-Pintado, N. J. Rodríguez-Fernández, Molecular gas chemistry in AGN. *Astron. Astrophys.* **419**, 897–912 (2004).
4. R. Meijerink, M. Spaans, F. P. Israel, Diagnostics of irradiated dense gas in galaxy nuclei. *Astron. Astrophys.* **461**, 793–811 (2007).
5. S. García-Burillo, F. Combes, A. Usero, S. Aalto, M. Krips, S. Viti, A. Alonso-Herrero, L. K. Hunt, E. Schinnerer, A. J. Baker, F. Boone, V. Casasola, L. Colina, F. Costagliola, A. Eckart, A. Fuente, C. Henkel, A. Labiano, S. Matín, I. Márquez, S. Muller, P. Planesas, C. R. Almeida, M. Spaans, L. J. Tacconi, P. P. van der Werf, Molecular line emission in NGC 1068 imaged with ALMA. I. An AGN-driven outflow in the dense molecular gas. *Astron. Astrophys.* **567**, A125 (2014).
6. A. Labiano, S. García-Burillo, F. Combes, A. Usero, R. Soria-Ruiz, J. P. López, A. Fuente, L. Hunt, R. Neri, Fueling the central engine of radio galaxies. *Astron. Astrophys.* **564**, A128 (2014).
7. L. R. Liu, J. D. Hood, Y. Yu, J. T. Zhang, N. R. Hutzler, T. Rosenband, K.-K. Ni, Building one molecule from a reservoir of two atoms. *Science* **360**, 900–903 (2018).
8. Y.-P. Chang, K. Długołęcki, J. Küpper, D. Rösch, D. Wild, S. Willitsch, Specific chemical reactivities of spatially separated 3-Aminophenol conformers with cold Ca^+ ions. *Science* **342**, 98–101 (2013).
9. P. Puri, M. Mills, C. Schneider, I. Simbotin, J. A. Montgomery Jr., R. Côté, A. G. Suits, E. R. Hudson, Synthesis of mixed hypermetallic oxide $BaOCa^+$ from laser-cooled reagents in an atom-ion hybrid trap. *Science* **357**, 1370–1375 (2017).
10. S. Willitsch, M. T. Bell, A. D. Gingell, S. R. Procter, T. P. Softley, Cold reactive collisions between laser-cooled ions and velocity-selected neutral molecules. *Phys. Rev. Lett.* **100**, 043203 (2008).
11. J. Deiglmayr, A. Göritz, T. Best, M. Weidemüller, R. Wester, Reactive collisions of trapped anions with ultracold atoms. *Phys. Rev. A* **86**, 043438 (2012).
12. F. H. J. Hall, S. Willitsch, Millikelvin reactive collisions between sympathetically cooled molecular ions and laser-cooled atoms in an ion-atom hybrid trap. *Phys. Rev. Lett.* **109**, 233202 (2012).
13. C. Savage, L. M. Ziurys, Ion chemistry in photon-dominated regions: Examining the $[HCO^+]/[HOC^+]/[CO^+]$ chemical network. *Astrophys J* **616**, 966–975 (2004).
14. L. M. Ziurys, A. J. Apponi, Confirmation of interstellar HOC^+: Reevaluating the $[HCO]^+/[HOC]^+$ abundance ratio. *Astrophys. J.* **455**, L73–L76 (1995).
15. J. Armijos-Abendaño, J. Martín-Pintado, E. López, M. Llerena, N. Harada, M. A. Requena-Torres, S. Martín, V. M. Rivilla, D. Riquelme, F. Aldas, On the effects of UV photons/X-Rays on the chemistry of the Sgr B2 cloud. *Astrophys. J.* **895**, 57 (2020).
16. A. Fuente, S. García-Burillo, A. Usero, M. Gerin, R. Neri, A. L. Faure, J. Bourlot, M. González-García, J. R. Rizzo, T. Alonso-Albi, J. Tennyson, On the chemistry and distribution of HOC^+ in M 82: More evidence for extnsive PDRs. *Astron. Astrophys.* **492**, 675–684 (2008).
17. A. Fuente, S. García-Burillo, M. Gerin, D. Teyssier, A. Usero, J. R. Rizzo, P. de Vicente, Photon-dominated chemistry in the nucleus of M82: Widespread HOC^+ emission in the inner 650 parsec disk. *Astrophys. J.* **619**, L155–L158 (2005).
18. S. Martín, J. Martín-Pintado, S. Viti, Photodissociation chemistry footprints in the starburst galaxy NGC 253. *Astrophys. J.* **706**, 1323–1330 (2009).

19. R. Aladro, S. König, S. Aalto, E. González-Alfonso, N. Falstad, S. Martín, S. Muller, S. García-Burillo, C. Henkel, P. van der Werf, E. Mills, J. Fischer, F. Costagliola, M. Krips, Molecular gas in the northern nucleus of Mrk 273: Physical and chemical properties of the disc and its outflow. *Astron. Astrophys.* **617**, A20 (2018).
20. J. Armijos-Abendaño, J. Martín-Pintado, M. A. Requena-Torres, S. Martín, A. Rodríguez-Franco, 3-mm spectral line survey of two lines of sight towards two typical cloud complexes in the Galactic Centre. *Mon. Not. R Astron. Soc.* **446**, 3842–3862 (2014).
21. R. C. Woods, C. S. Gudeman, R. L. Dickman, P. F. Goldsmith, G. R. Huguenin, W. M. Irvine, A. Hjalmarson, L.-A. Nyman, H. Olofsson, The $[HCO^+]/[HOC^+]$ abundance ratio in molecular clouds. 270, 583–588 (1983).
22. C. G. Freeman, M. J. McEwan, A selected-ion flow tube study of the $C^+ + H_2O$ reaction. *Int. J. Mass Spectrom. Ion Process* **75**, 127–131 (1987).
23. J. R. Flores, A. B. González, The role of the excited electronic states in the $C^+ + H_2O$ reaction. *J. Chem. Phys.* **128**, 144310 (2008).
24. Å. Larson, A. E. Orel, Electronic resonant states of HCO and HOC. *Phys. Rev. A* **80**, 062504 (2009).
25. D. M. Sonnenfroh, R. A. Curtis, J. M. Farrar, Collision complex formation in the reaction of C^+ with H_2O. *J. Chem. Phys.* **83**, 3958–3964 (1985).
26. J. B. Marquette, B. R. Rowe, G. Dupeyrat, G. Poissant, C. Rebrion, Ion—Polar-molecule reactions: A CRESU study of He^+, C^+, $N^+ + H_2O$, NH_3 at 27, 68 and 163 K. *Chem. Phys. Lett.* **122**, 431–435 (1985).
27. J. O. Martinez Jr., N. B. Betts, S. M. Villano, N. Eyet, T. P. Snow, V. M. Bierbaum, Gas phase study of C^+ reactions of interstellar relevance. *Astrophys. J.* **686**, 1486–1492 (2008).
28. D. J. Defrees, A. D. McLean, E. Herbst, Calculations concerning the HCO^+/HOC^+ abundance ratio in dense interstellar clouds. *Astrophys. J.* **279**, 322–334 (1984).
29. Y. Ishikawa, R. C. Binning Jr., T. Ikegami, Direct ab initio molecular dynamics study of C^++H_2O. *Chem. Phys. Lett.* **343**, 413–419 (2001).
30. M. A. Smith, S. Schlemmer, J. von Richthofen, D. Gerlich, $HOC^+ + H_2$ isomerization rate at 25 K: Implications for the observed $[HCO^+]/[HOC^+]$ ratios in the interstellar medium. *Astrophys. J.* **578**, L87–L90 (2002).
31. B. R. Rowe, J. B. Marquette, CRESU studies of ion/molecule reactions. *Int. J. Mass Spectrom. Ion Process.* **80**, 239–254 (1987).
32. D. Gerlich, M. Smith, Laboratory astrochemistry: Studying molecules under inter- and circumstellar conditions. *Phys. Scr.* **73**, C25–C31 (2005).
33. W. Paul, Electromagnetic traps for charged and neutral particles. *Rev. Mod. Phys.* **62**, 531–540 (1990).
34. T. Yang, A. Li, G. K. Chen, C. Xie, A. G. Suits, W. C. Campbell, H. Guo, E. R. Hudson, Optical control of reactions between water and laser-cooled Be^+ ions. *J. Phys. Chem. Lett.* **9**, 3555–3560 (2018).
35. G. K. Chen, C. Xie, T. Yang, A. Li, A. G. Suits, E. R. Hudson, W. C. Campbell, H. Guo, Isotope-selective chemistry in the $Be^+(^2S_{1/2})$ + HOD → $BeOD^+/BeOH^+$ + H/D reaction. *Phys. Chem. Chem. Phys.* **21**, 14005–14011 (2019).
36. D. J. Wineland, W. M. Itano, Laser cooling of atoms. *Phys. Rev. A* **20**, 1521–1540 (1979).
37. E. R. Hudson, Sympathetic cooling of molecular ions with ultracold atoms. *EPJ Tech. Instrum.* **3**, 8 (2016).
38. E. R. Hudson, Method for producing ultracold molecular ions. *Phys. Rev. A* **79**, 032716 (2009).
39. Z. Fang, V. H. S. Kwong, J. Wang, W. H. Parkinson, Measurements of radiative-decay rates of the $2s^22p(^2P^0)$-$2s2p^2(^4P)$ intersystem transition of C^+. *Phys. Rev. A* **48**, 1114–1122 (1993).
40. D. Patterson, J. Rasmussen, J. M. Doyle, Intense atomic and molecular beams via neon buffer-gas cooling. *New J. Phys.* **11**, 055018 (2009).
41. S. J. Schowalter, K. Chen, W. G. Rellergert, S. T. Sullivan, E. R. Hudson, An integrated ion trap and time-of-flight mass spectrometer for chemical and photo-reaction dynamics studies. *Rev. Sci. Instrum.* **83**, 043103 (2012).
42. C. Schneider, S. J. Schowalter, K. Chen, S. T. Sullivan, E. R. Hudson, Laser-Cooling-Assisted mass spectrometry. *Phys. Rev. Applied* **2**, 034013 (2014).
43. G. Mauclaire, J. Lemaire, M. Heninger, S. Fenistein, D. C. Parent, R. Marx, Radiative lifetimes for an ion of astrophysical interest: HCO^+. *Int. J. Mass Spectrom. Ion Process.* **149-150**, 487–497 (1995).
44. N. G. Adams, D. Smith, D. Grief, Reactions of H_nCO^+ ions with molecules at 300 K. *Int. J. Mass Spectrom. Ion Phys.* **26**, 405–415 (1978).
45. A. J. Chalk, L. Radom, Proton-Transport catalysis: A systematic study of the rearrangement of the isoformyl cation to the formyl cation. *J. Am. Chem. Soc.* **119**, 7573–7578 (1997).
46. X. Hu, W. L. Hase, T. Pirraglia, Vectorization of the general Monte Carlo classical trajectory program VENUS. *J. Comput. Chem.* **12**, 1014–1024 (1991).
47. Q. Yao, C. Xie, H. Guo, Competition between proton transfer and proton isomerization in the $N_2 + HOC^+$ reaction on an Ab Initio-based global potential energy surface. *J. Phys. Chem. A* **123**, 5347–5355 (2019).
48. D. McElroy, C. Walsh, A. J. Markwick, M. A. Cordiner, K. Smith, T. J. Millar, The UMIST database for astrochemistry 2012. *Astron. Astrophys.* **550**, A36 (2013).
49. M. Röllig, N. P. Abel, T. Bell, F. Bensch, J. Black, G. J. Ferland, B. Jonkheid, I. Kamp, M. J. Kaufman, J. Le Bourlot, F. Le Petit, R. Meijerink, O. Morata, V. Ossenkopf, E. Roueff, G. Shaw, M. Spaans, A. Sternberg, J. Stutzki, W.-F. Thi, E. F. van Dishoeck, P. A. M. van Hoof, S. Viti, M. G. Wolfire, A photon dominated region code comparison study. *Astron. Astrophys.* **467**, 187–206 (2007).
50. N. R. Hutzler, H.-I. Lu, J. M. Doyle, The buffer gas beam: An intense, cold, and slow source for atoms and molecules. *Chem. Rev.* **112**, 4803–4827 (2012).
51. P.-Y. Zhao, Z.-X. Xiong, L. Jie, L.-X. He, B.-L. Lu, Magneto-Optical Trapping of Ytterbium Atoms with a 398.9 nm Laser. *Chin. Phys. Lett.* **25**, 3631–3634 (2008).
52. C. G. Freeman, J. S. Knight, J. G. Love, M. J. McEwan, The reactivity of HOC^+ and the proton affinity of CO at O. *Int. J. Mass Spectrom. Ion Process.* **80**, 255–271 (1987).
53. V. G. Anicich, Evaluated bimolecular ion-molecule gas phase kinetics of positive ions for use in modeling planetary atmospheres, cometary comae, and interstellar clouds. *J. Phys. Chem. Ref. Data Monogr.* **22**, 1469–1569 (1993).
54. NIST, Computational Chemistry Comparison and Benchmark Database, NIST Standard Reference Database Number 101, R. D. Johnson III, Ed. Release 21, August 2020; http://cccbdb.nist.gov/. DOI:10.18434/T47C7Z.
55. G. Knizia, T. B. Adler, H.-J. Werner, Simplified CCSD(T)-F12 methods: Theory and benchmarks. *J. Chem. Phys.* **130**, 054104 (2009).
56. K. A. Peterson, T. B. Adler, H.-J. Werner, Systematically convergent basis sets for explicitly correlated wavefunctions: The atoms H, He, B–Ne, and Al–Ar. *J. Chem. Phys.* **128**, 084102 (2008).
57. A. J. Stone, *The Theory of Intermolecular Forces* (Oxford Univ. Press, ed. 2, 2013).
58. A. D. Buckingham, Permanent and induced molecular moments and long-range intermolecular forces. *Adv. Chem. Phys.* **12**, 107–142 (1967).
59. B. Jiang, J. Li, H. Guo, Potential energy surfaces from high fidelity fitting of ab initio points: The permutation invariant polynomial-neural network approach. *Int. Rev. Phys. Chem.* **35**, 479–506 (2016).
60. J.-i. Yamamoto, Ab initio molecular dynamics simulation on $H_2O + C^+$ reaction. *J. Mol. Struct.* **957**, 55–60 (2010).
61. R. Wester, U. Hechtfischer, L. Knoll, M. Lange, J. Levin, M. Scheffel, D. Schwalm, A. Wolf, A. Baer, Z. Vager, D. Zajfman, M. Mladenović, S. Schmatz, Relaxation dynamics of deuterated formyl and isoformyl cations. *J. Chem. Phys.* **116**, 7000–7011 (2002).
62. J. A. DeVine, M. L. Weichman, B. Laws, J. Chang, M. C. Babin, G. Balerdi, C. Xie, C. L. Malbon, W. C. Lineberger, D. R. Yarkony, R. W. Field, S. T. Gibson, J. Ma, H. Guo, D. M. Neumark, Encoding of vinylidene isomerization in its anion photoelectron spectrum. *Science* **358**, 336–339 (2017).
63. M. Mladenović, S. Schmatz, Theoretical study of the rovibrational energy spectrum and the numbers and densities of bound vibrational states for the system HCO^+/HOC^+. *J. Chem. Phys.* **109**, 4456–4470 (1998).

Acknowledgments: The authors are indebted to C. Schneider and D. Patterson for helpful technical advice. **Funding:** This work was supported by the Air Force Office of Scientific Research grant nos. FA9550-16-1-0018 and FA9550-18-1-0413. A.L. acknowledges the support of the Key Science and Technology Innovation Team of Shanxi Province (2017KCT-37). H.G. thanks the Alexander von Humboldt Foundation for a Humboldt Research Award. **Author contributions:** T.Y. and G.K.C. took the experimental data. A.L., Q.Y., and H.G. performed the theory calculations. T.Y., G.K.C., A.G.S., E.R.H., and W.C.C. designed the experiment and analyzed the experimental data. All authors participated in the preparation of the manuscript. **Competing interests:** The authors declare that they have no competing interests. **Data and materials availability:** All data needed to evaluate the conclusions in the paper are present in the paper and/or Supplementary Materials. Additional data related to this paper may be requested from the authors.

Submitted 19 August 2020
Accepted 12 November 2020
Published 6 January 2021
10.1126/sciadv.abe4080

Citation: T. Yang, A. Li, G. K. Chen, Q. Yao, A. G. Suits, H. Guo, E. R. Hudson, W. C. Campbell, Isomer-specific kinetics of the $C^+ + H_2O$ reaction at the temperature of interstellar clouds. *Sci. Adv.* **7**, eabe4080 (2021).